LIQUID CRYSTALS, 2000, VOL. 27, NO. 9, 1151–1160

Molecular shape and flexoelectricity

JEFFREY L. BILLETER and ROBERT A. PELCOVITS*
Department of Physics, Brown University, Providence, RI 02912, USA

(*Received 22 October 1999; in final form 16 February 2000; accepted 22 February 2000*)

Monte Carlo simulations were performed of systems of wedge-shaped objects formed from Gay–Berne ellipsoids joined to Lennard–Jones spheres. We studied two different wedge shapes, one more asymmetric than the other. The bend and splay flexoelectric coefficients were measured in the isotropic and smectic phases using linear response theory, and found to be negligibly small in the isotropic phase. We found a close connection between the properties of the intermolecular potential and the flexoelectric coefficients measured in the smectic phase. In particular, negligible bend coefficients were found for both shapes and a larger magnitude of the splay coefficient for the more prominent wedge, in accord with Meyer's original mechanism for flexoelectricity. The less prominent wedge produced a splay flexoelectric coefficient with the opposite sign due to the attractive tail of the intermolecular potential and the relative narrowness of the molecular head.

1. Introduction

In the flexoelectric effect a director deformation produces an electrical polarization, similar to the phenomenon of piezoelectricity in solid crystals. The flexoelectric effect was first proposed by Meyer [1] who considered asymmetric molecules either wedge-shaped with longitudinal dipole moments or 'banana' shaped with transverse dipoles. In the absence of a director deformation, the packing of the molecules is similar to that of ellipsoidal-shaped or rod-like molecules (the additional asymmetries of the molecules have negligible effect) and the average polarization is zero. However, when a splay is imposed upon a system of wedges or a bend upon a system of bananas, the preferred packing of the molecules results in a net alignment of dipoles leading to an overall polarization of the medium (see figures 1 and 2). Alternatively, an applied electric field which aligns the dipoles induces a splay or bend in the appropriately shaped system—this is sometimes called the inverse flexoelectric effect. In either case, the net polarization $\mathbf{P}$ and the elastic deformations are related by the flexoelectric coefficients e_{11} and e_{33} introduced by Meyer through the following linear response relation:

$$\mathbf{P} = e_{11}\hat{\mathbf{n}}(\nabla \quad \hat{\mathbf{n}}) + e_{33}\hat{\mathbf{n}} \times (\nabla \times \hat{\mathbf{n}}) \qquad (1)$$

where $\hat{\mathbf{n}}$ is the director. The first term on the right hand side of this equation corresponds to splay flexoelectricity (relevant for wedges) and the second term to bend flexoelectricity (relevant for bananas).

*Author for correspondence;
e-mail: pelcovits@physics.brown.edu

Subsequent to Meyer's work, Prost and Marcerou [2] proposed a flexoelectric mechanism based on molecular quadrupoles requiring neither the shape asymmetries nor the dipole moments of Meyer's original argument. Rather, molecular quadrupoles allow uneven charge distributions leading to polarizations in any given volume when a splay is imposed (see figure 3).

Both the Meyer dipole and the Prost and Marcerou quadrupole mechanisms have been observed experimentally [3–7]. Typically, the flexoelectric coefficients are measured over a range of temperature in the nematic phase and their variation compared with that of the nematic order parameter S. Although it has been shown that for both the dipole and quadrupole mechanisms there are contributions to the flexoelectric coefficients involving several powers of S, Marcerou and Prost used the dominant contributions—S for the quadrupole mechanism and S^2 for the dipole mechanism—in the analysis of their experimental data [4]. They found flexoelectric coefficients proportional to S for symmetric, non-polar molecules, clearly demonstrating the quadrupole mechanism. Quadratic variation with S was seen for banana-shaped molecules with strong, transverse dipole moments.

In the smectic A phase, an additional flexoelectric coefficient arises, representing the coupling between the net polarization and variations in the smectic layer spacing [6, 8–10]. Specifically, there is an additional contribution to the right-hand side of equation (1) proportional to $(\partial^2 u/\partial z^2)\hat{\mathbf{z}}$, where u is the displacement of the smectic layers whose normals are parallel to the $\hat{\mathbf{z}}$ axis. Prost and Pershan [6] found this additional term

Liquid Crystals ISSN 0267-8292 print/ISSN 1366-5855 online © 2000 Taylor & Francis Ltd
http://www.tandf.co.uk/journals

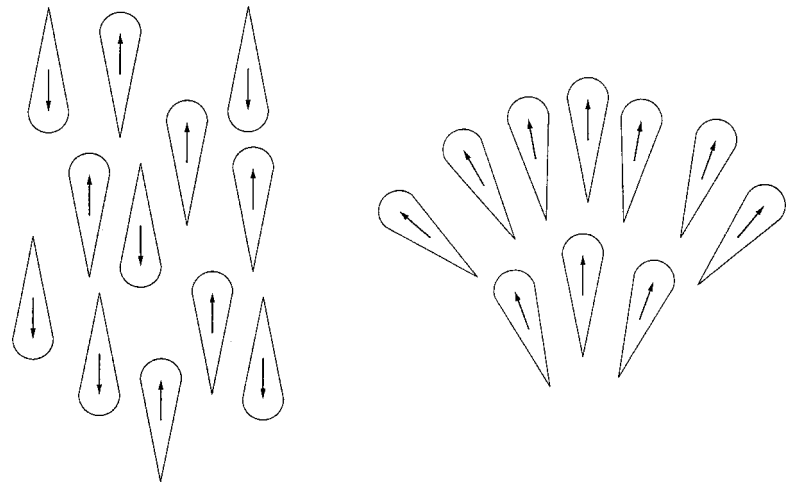

Figure 1. (*a*) Wedges with longitudinal dipoles under normal nematic conditions; there is no splay and no net polarization. (*b*) Under an applied splay, the preferred wedge alignment results in a net polarization; alternatively, an applied field induces a splay due to the wedge shape of the molecules.

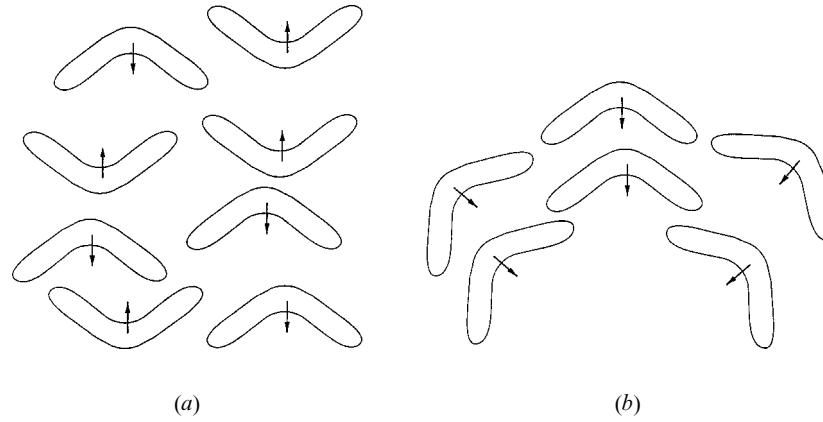

Figure 2. (*a*) 'Bananas' with transverse dipoles under normal nematic conditions; there is no bend and no net polarization. (*b*) Under an applied bend, the preferred banana alignment results in a net polarization; alternatively, an applied field induces a bend due to the banana shape of the molecules.

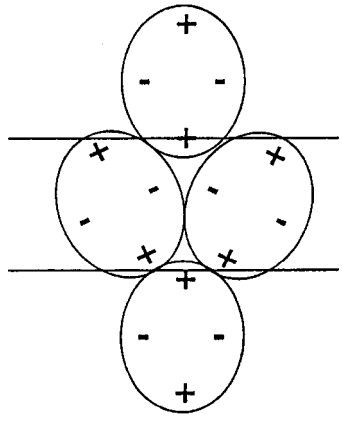

Figure 3. Quadrupoles with a splay imposed. Within the central 'layer', plus charges from above are allowed to enter, while plus charges below are expelled, leading to a net polarization upwards.

to be negligible experimentally. The flexoelectricity of the smectic C phase involves a total of 14 coefficients and is discussed in [9].

A systematic method for calculating flexoelectric coefficients based on molecular shape and multipole properties would be very valuable. Mean-field theories [2, 11–14] do not consider the short range fluctuations in molecular alignment which can be quite important. Computer simulations offer a way to assess the molecular origins of flexoelectricity. In particular, simulations can focus strictly on Meyer's packing ideas without the complication of dipolar interactions which could lead to antiparallel alignment of side-by-side molecules. To date, only one simulation study [15] of flexoelectricity has been carried out. In this study the flexoelectric coefficients were evaluated for wedge-shaped molecules interacting via a generalized Gay–Berne potential [16]. The molecules were modelled in this study (as well as in ours) by a Gay–Berne ellipsoid with a Lennard–Jones sphere attached near one end (see figure 4). Two sets of parameters were considered in [15], one with a slightly more pronounced wedge shape than the other. The flexoelectric coefficients were evaluated using microscopic expressions based on density functional theory,

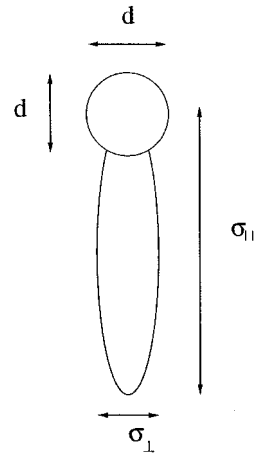

Figure 4. Illustration of the basic geometric parameters of the wedge-shaped molecule composed of a rod and sphere.

and a larger value of e_{11} was obtained for the more pronounced wedge. The bend flexoelectric coefficient was nearly zero, in agreement with Meyer's suggestion that bend flexoelectricity should not appear in a system of wedges.

In this paper we consider a similar model but extend the study in several ways. First, we evaluate the flexoelectric coefficients using linear response theory and the fluctuation–dissipation theorem, which provide a computationally simpler and more direct means of evaluation compared with density functional theory. Second, we consider two model sets of molecular parameters, one representing a molecule with significantly more asymmetry than either molecule considered in [15]. By exploring the intermolecular potentials for our two sets of parameters we find that the less prominent wedges (similar to the less prominent ones considered in [15]) prefer to align with their larger ends tilted *toward* each other (because of the short range attractive interaction), while the more prominent wedges prefer to align with their larger ends tilted *away* from each other (in this case the repulsive hard core interaction dominates). These opposing tendencies in turn lead to opposite signs of the splay flexoelectric coefficients. While Meyer's original argument considered only repulsive hard core interactions, it is consistent with his ideas to expect this difference in signs if attractive forces are also included. As in [15], and also consistent with Meyer's ideas, we find a negligible value of the bend flexoelectric coefficient.

The outline of this paper is as follows. In the next section we present the details of our modelling of wedge-shaped molecules. Section 3 discusses the linear response theory used to measure the flexoelectric coefficients in our simulation. Our results are presented in § 4 and we offer some concluding remarks in the final section.

2. Molecular shape modelling

Using an approach similar to that of [15] we constructed a wedge-shaped molecule from a standard Gay–Berne ellipsoid (or rod) with a sphere added near one end (see figure 4). The net interaction potential between two wedge-shaped molecules labelled 1 and 2 then consists of four terms, namely

$$U_{\mathrm{tot}} = U_{\mathrm{rod1\text{-}rod2}} + U_{\mathrm{sphere1\text{-}sphere2}} + U_{\mathrm{rod1\text{-}sphere2}} + U_{\mathrm{sphere1\text{-}rod2}} \tag{2}$$

where $U_{\mathrm{rod1\text{-}rod2}}$ is given by the original Gay–Berne potential [17]:

$$U_{\mathrm{rod1\text{-}rod2}}(\hat{\mathbf{u}}_1, \hat{\mathbf{u}}_2, \mathbf{r}) = 4\varepsilon(\hat{\mathbf{u}}_1, \hat{\mathbf{u}}_2, \hat{\mathbf{r}}) \times \left\{ \left[\frac{\sigma_{\mathrm{o}}}{r - \sigma(\hat{\mathbf{u}}_1, \hat{\mathbf{u}}_2, \hat{\mathbf{r}}) + \sigma_{\mathrm{o}}} \right]^{12} - \left[\frac{\sigma_{\mathrm{o}}}{r - \sigma(\hat{\mathbf{u}}_1, \hat{\mathbf{u}}_2, \hat{\mathbf{r}}) + \sigma_{\mathrm{o}}} \right]^{6} \right\} \tag{3}$$

where $\hat{\mathbf{u}}_1, \hat{\mathbf{u}}_2$ give the orientations of the long axes of rods 1 and 2, respectively, and $\mathbf{r} = \mathbf{r}_1 - \mathbf{r}_2$, with the centres of the rods located at positions $\mathbf{r}_1$ and $\mathbf{r}_2$. The parameter $\sigma(\hat{\mathbf{u}}_1, \hat{\mathbf{u}}_2, \hat{\mathbf{r}})$ is the separation between the rods at which the potential vanishes, and thus represents the shape of the rods. Its explicit form is

$$\sigma(\hat{\mathbf{u}}_1, \hat{\mathbf{u}}_2, \hat{\mathbf{r}}) = \sigma_{\mathrm{o}} \left\{ 1 - \frac{1}{2}\chi \left[\frac{(\hat{\mathbf{r}}\ \hat{\mathbf{u}}_1 + \hat{\mathbf{r}}\ \hat{\mathbf{u}}_2)^2}{1 + \chi(\hat{\mathbf{u}}_1\ \hat{\mathbf{u}}_2)} + \frac{(\hat{\mathbf{r}}\ \hat{\mathbf{u}}_1 - \hat{\mathbf{r}}\ \hat{\mathbf{u}}_2)^2}{1 - \chi(\hat{\mathbf{u}}_1\ \hat{\mathbf{u}}_2)} \right] \right\}^{-1/2} \tag{4}$$

where $\sigma_{\mathrm{o}} = \sigma_{\perp}$ (defined below) and χ is

$$\chi = [(\sigma_{\parallel}/\sigma_{\perp})^2 - 1]/[(\sigma_{\parallel}/\sigma_{\perp})^2 + 1]. \tag{5}$$

Here $\sigma_{\parallel}$ is the separation between two rods when they are oriented end-to-end with $U_{\mathrm{rod1\text{-}rod2}} = 0$, and $\sigma_{\perp}$ is the corresponding separation when the two rods are side-by-side. The well depth $\varepsilon(\hat{\mathbf{u}}_1, \hat{\mathbf{u}}_2, \hat{\mathbf{r}})$, representing the anisotropy of the attractive interactions, is written as

$$\varepsilon(\hat{\mathbf{u}}_1, \hat{\mathbf{u}}_2, \mathbf{r}) = \varepsilon_{\mathrm{o}} \varepsilon^{\nu}(\hat{\mathbf{u}}_1, \hat{\mathbf{u}}_2) \varepsilon'^{\mu}(\hat{\mathbf{u}}_1, \hat{\mathbf{u}}_2, \hat{\mathbf{r}}) \tag{6}$$

where

$$\varepsilon(\hat{\mathbf{u}}_1, \hat{\mathbf{u}}_2) = [1 - \chi^2(\hat{\mathbf{u}}_1\ \hat{\mathbf{u}}_2)^2]^{-1/2} \tag{7}$$

and

$$\varepsilon'(\hat{\mathbf{u}}_1, \hat{\mathbf{u}}_2, \hat{\mathbf{r}}) = 1 - \frac{1}{2}\chi' \left[\frac{(\hat{\mathbf{r}}\ \hat{\mathbf{u}}_1 + \hat{\mathbf{r}}\ \hat{\mathbf{u}}_2)^2}{1 + \chi'(\hat{\mathbf{u}}_1\ \hat{\mathbf{u}}_2)} + \frac{(\hat{\mathbf{r}}\ \hat{\mathbf{u}}_1 - \hat{\mathbf{r}}\ \hat{\mathbf{u}}_2)^2}{1 - \chi'(\hat{\mathbf{u}}_1\ \hat{\mathbf{u}}_2)} \right] \tag{8}$$

with χ' defined in terms of $\varepsilon_{\parallel}$ and $\varepsilon_{\perp}$, the end-to-end and side-by-side well depths, respectively, as

$$\chi' = [1 - (\varepsilon_{\parallel}/\varepsilon_{\perp})^{1/\mu}]/[1 + (\varepsilon_{\parallel}/\varepsilon_{\perp})^{1/\mu}]. \tag{9}$$

We measure all of our physical quantities in reduced units in terms of the energy scale ε_o and the length scale σ_o. For the adjustable parameters appearing in equations (6), (8) and (9), we used the values originally proposed by Gay and Berne [17]: $\mu = 2$, $\nu = 1$, and $\varepsilon_\perp/\varepsilon_\parallel = 5$. Our choices for the rod shape parameters $\sigma_\parallel$ and $\sigma_\perp$ are discussed below.

The interaction $U_{\text{sphere1-sphere2}}$ is given by the ordinary Lennard–Jones potential:

$$U_{\text{sphere1-sphere2}}(\mathbf{r}) = 4\varepsilon_o\left[\left(\frac{d}{r}\right)^{12} - \left(\frac{d}{r}\right)^{6}\right] \qquad (10)$$

where d is the separation between the two spheres at which the potential $U_{\text{sphere1-sphere2}}$ vanishes; i.e. it is a measure of the diameter of the sphere. The relative position vector $\mathbf{r}$ is measured from the centre of sphere 1 to the centre of the sphere 2.

The interaction between the rod-like part of one molecule and the sphere of the other molecule, $U_{\text{rod1-sphere2}}$, is given by a Gay–Berne potential generalized to mimic the interaction between non-equivalent particles [16]. The range parameter $\sigma_{rs}(\hat{\mathbf{u}}_1, \mathbf{r}_{12})$ and the energy parameter $\varepsilon_{rs}(\hat{\mathbf{u}}_i, \hat{\mathbf{u}}_j)$ used in this potential are generalizations of the corresponding parameters in equations (4) and (6), namely [16]:

$$\sigma_{rs}(\hat{\mathbf{u}}_1, \hat{\mathbf{r}}) = \sigma_o^{rs}(1 - \chi_{rs}(\hat{\mathbf{r}}\ \ \hat{\mathbf{u}}_1))^{-1/2} \qquad (11)$$

and

$$\varepsilon_{rs}(\hat{\mathbf{u}}_1, \hat{\mathbf{r}}) = 1 \qquad (12)$$

with χ_{rs} defined as

$$\chi_{rs} = \frac{\sigma_\parallel^2 - \sigma_\perp^2}{\sigma_\parallel^2 + d^2} \qquad (13)$$

and

$$\sigma_o^{rs} = \frac{1}{\sqrt{2}}(\sigma_\perp^2 + d^2)^{1/2}. \qquad (14)$$

In the rod–sphere potential the relative position vector $\mathbf{r}$ is measured for the centre of the rod to the centre of the sphere.

We performed simulations for two sets of molecular parameters: a slightly wedge-shaped object with $\sigma_\perp = 1.0$, $\sigma_\parallel = 2.6$, $d = 0.94$, and a more prominent wedge with parameters $\sigma_\perp = 1.0$, $\sigma_\parallel = 2.4$, $d = 1.3$. In the former case the centre of the sphere was located at a distance $D = 1.3$ from the centre of the rod, and at a distance $D = 1.2$ in the latter case. In terms of the steric dipole moment $p^* = (4\pi/3)(d/2)^3 D$ introduced in [15], our parameters correspond to values of P^* of 0.565 and 1.38 respectively (in [15] systems with dipole moments of 0.524 and 0.662 were studied).

To ascertain the effective shape of the composite rod–sphere molecule we computed equipotential contours (with contour values close to zero). The contour plots are shown for the two sets of parameters in figures 5 and 6, clearly indicating a wedge-like shape. To explore the interaction and local packing of the molecules we computed the depths of the potential wells of U_{tot} for several different relative orientations of a pair of molecules with relative tilt θ. The results for the two sets of molecular parameters are shown in figures 7 and 8. For the purposes of comparison corresponding curves for the original Gay–Berne potential $U_{\text{rod1-rod2}}$ are shown in figure 9.

Comparing figures 7 and 8 with figure 9, we note that in the twist (*b*) and bend (*c*) configurations there is left–right symmetry about 180°, which is to be expected given that all three molecular shapes are rotationally symmetric about the long molecular axis. Furthermore, this symmetry leads, as expected, to a zero bend flexoelectric coefficient; twist will never produce a flexoelectric polarization. On the other hand, for the splay configuration, figures 7(*a*) and 8(*a*), the wedges do not exhibit the left–right tilt symmetry ($\theta \to \theta + 180°$) seen in the twist and bend configurations as well as the splay configuration, figure 9(*a*), of the Gay–Berne case. This result is not surprising: tilting the larger end of one wedge *away* from the larger end of another wedge (corresponding to $\theta < 180°$ in the figures) should yield a different energy than tilting the larger ends *toward* each other. More importantly, for each set of wedge parameters there is an absolute minimum in the potential energy corresponding to a finite but small splay angle. For the more prominent wedge shape, figure 8(*a*), this angle is approximately 10°; i.e. the pair of wedges prefer to align with their larger ends tilted away from each other. For the less prominent wedge shape, figure 7(*a*), the angle corresponding to the absolute minimum is nearly 360°; i.e. the wedges prefer to align with their larger ends tilted *toward* each other. As we shall see below, this difference yields flexoelectric coefficients of opposite signs for the two molecular shapes. While it might seem surprising at first glance that the less prominent wedges tilt toward each other, given the attractive interaction between two spheres and the fact that $d < \sigma_\perp$, in this case it is a reasonable result. For the more prominent wedges the larger repulsive core of the spheres leads to the expected tilting of the larger ends away from each other.

While the absolute minima of the pair potentials for the two sets of wedge parameters correspond to non-zero splay, note that this state is only slightly preferred over the aligned state, $\theta = 0°$, for the parameters of figure 7(*a*) and the antiparallel aligned state, $\theta = 180°$, for the more prominent wedge of figure 8(*a*). There

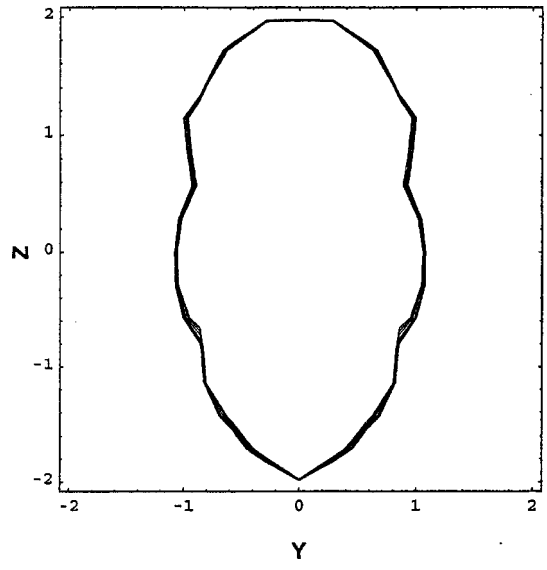

(*a*)

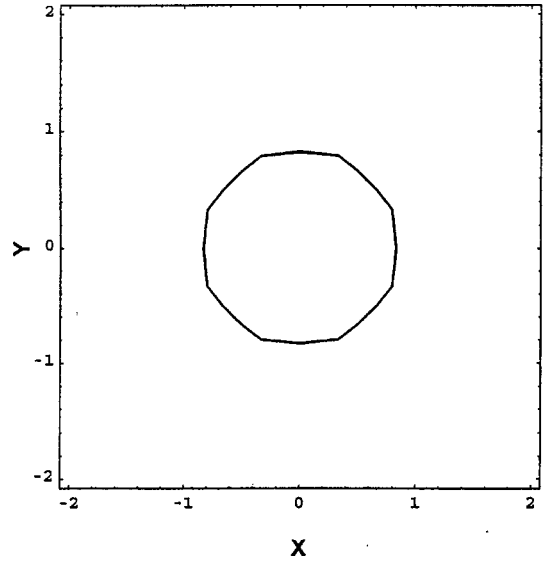

(*b*)

Figure 5. Potential energy contours showing the shape of the rod–sphere composite with parameters $\sigma_\perp = 1.0$, $\sigma_\parallel = 2.6$, $d = 0.94$: (*a*) side view showing wedge-like asymmetry; (*b*) top view showing axial symmetry. The top view contours are not completely circular due to a finite number of sample points. The side view data were generated by fixing one wedge in the *yz* plane as shown, while a second wedge pointing up out of the plane and with its narrow end just touching the plane 'scanned' across the first wedge. For the top view data, both wedges were parallel; one remained fixed while the other was moved around the first in the same plane.

is also a substantial subsidiary potential minimum for antiparallel slightly wedge-shaped molecules. In our simulations in the absence of an external electric field

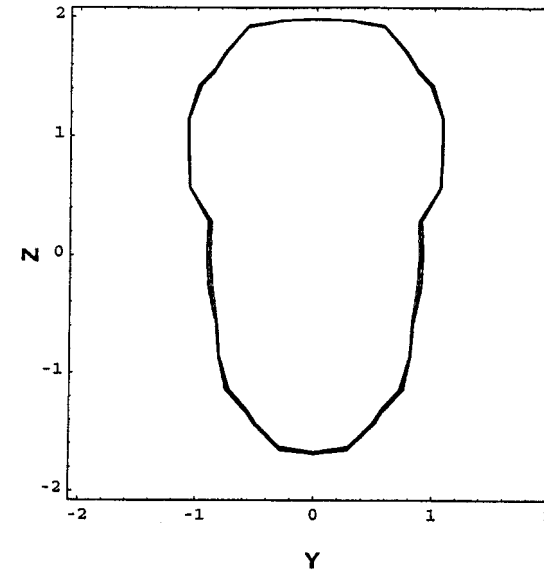

Figure 6. Potential energy contours showing the shape of the rod–sphere composite for a more prominent wedge with parameters $\sigma_\perp = 1.0$, $\sigma_\parallel = 2.4$, $d = 1.3$.

of a system of 256 wedge-shaped molecules using both sets of molecular parameters, we found, as expected on symmetry grounds, no net spontaneous splay or electric polarization (assuming molecular dipole moments parallel to the long axis of the wedge). However, if an electric field were applied to the system of prominent wedges, we would expect the potential well corresponding to non-zero splay to become deeper relative to that of the antiparallel state $\theta = 180°$, leading to splay flexoelectricity. For the slightly wedge-shaped objects of figure 7, the shallowness of the well corresponding to non-zero splay makes it less obvious that splay flexoelectricity will exist. However, in our simulations we do in fact splay flexoelectricity in this case, albeit smaller than in the case of the more prominent wedges and with the opposite sign.

We now turn to a discussion of how to extract the flexoelectric coefficients from our simulations.

3. Calculation of flexoelectric coefficients

To measure flexoelectric coefficients in this simulation, we used the linear response theory of Nemtsov and Osipov [18]. The flexoelectric coefficients in this method are related to the response function of the system to an orientational stress. Using the fluctuation-dissipation theorem, the response function can be found from correlation functions of the polarization density and the orientational stress tensor. The latter tensor is conjugate to the orientational strain which yields flexoelectricity. Thus, a calculation of the relevant correlation functions yields the flexoelectric coefficients.

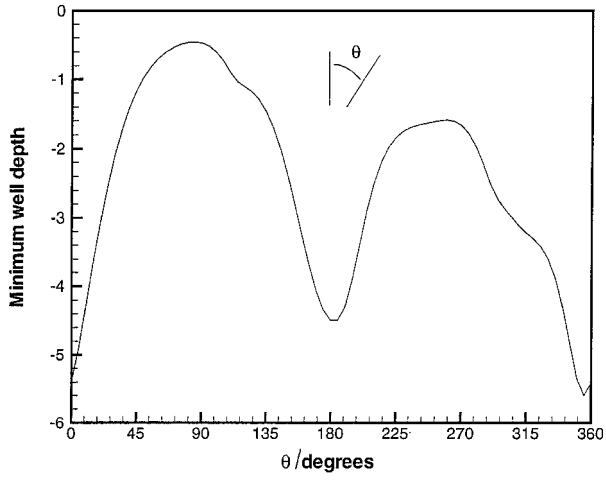

(*a*)

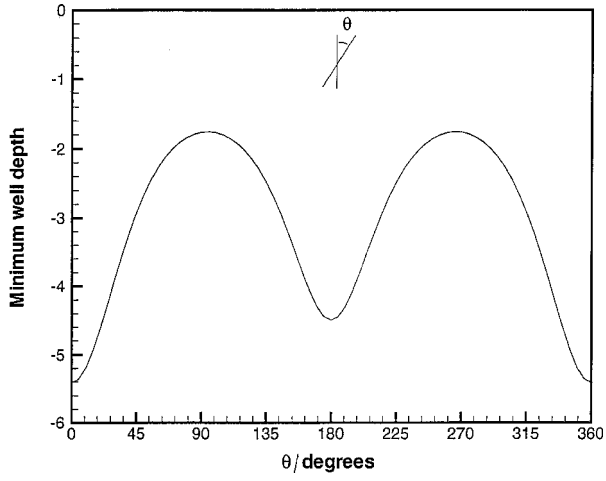

(*b*)

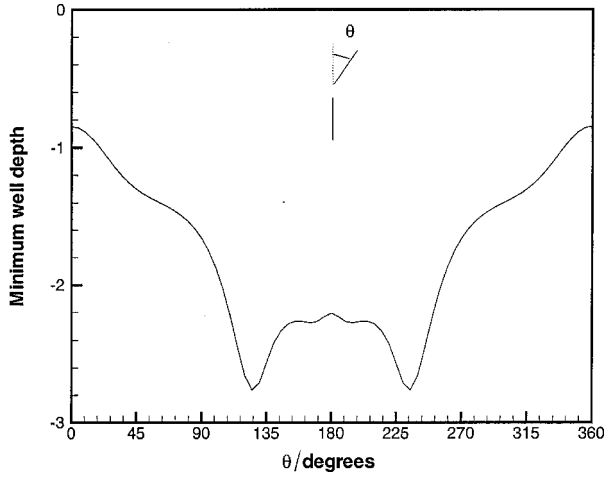

(*c*)

Figure 7. Minimum well depths (calculated as a function of molecular separation) for molecular parameters $\sigma_{\perp} = 1.0$, $\sigma_{\parallel} = 2.6$, $d = 0.94$ for various relative orientations as shown: (*a*) splay, (*b*) twist and (*c*) bend configurations.

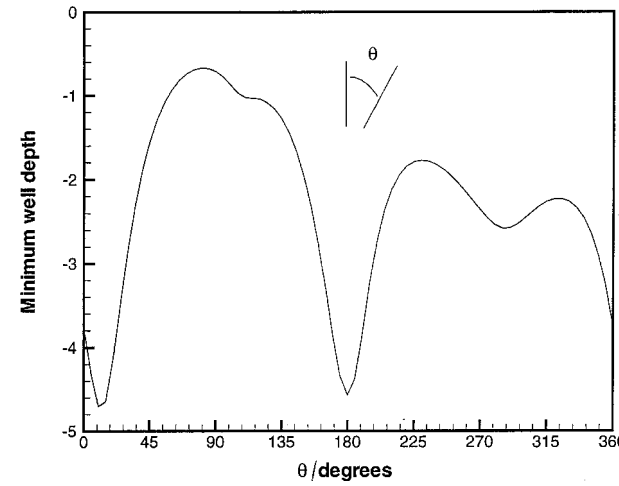

(*a*)

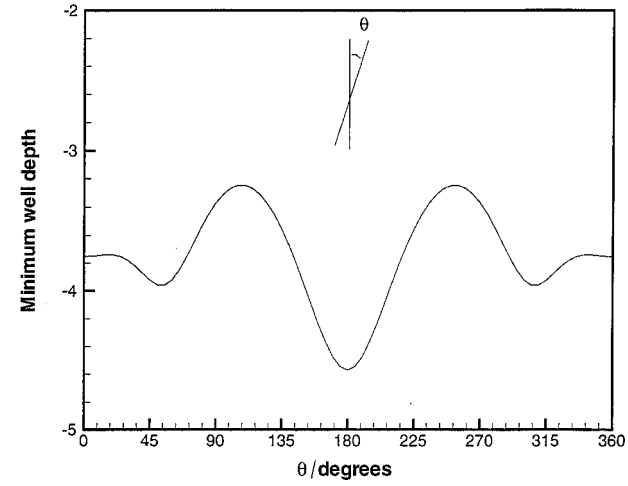

(*b*)

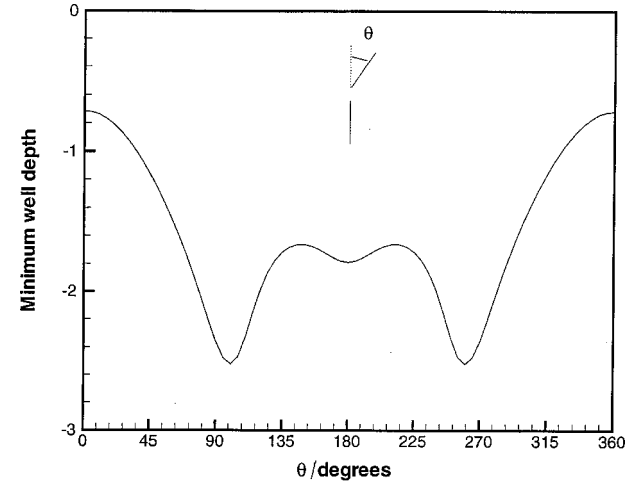

(*c*)

Figure 8. The same as figure 7 but for the more prominent wedges shown in figure 6, with parameters $\sigma_{\perp} = 1.0$, $\sigma_{\parallel} = 2.4$, $d = 1.3$.

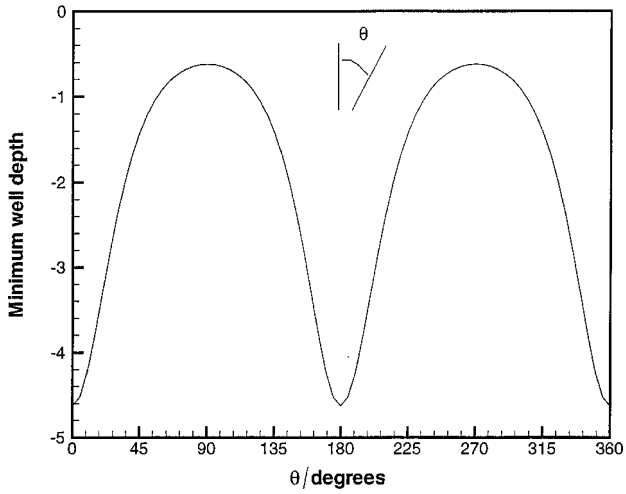

(*a*)

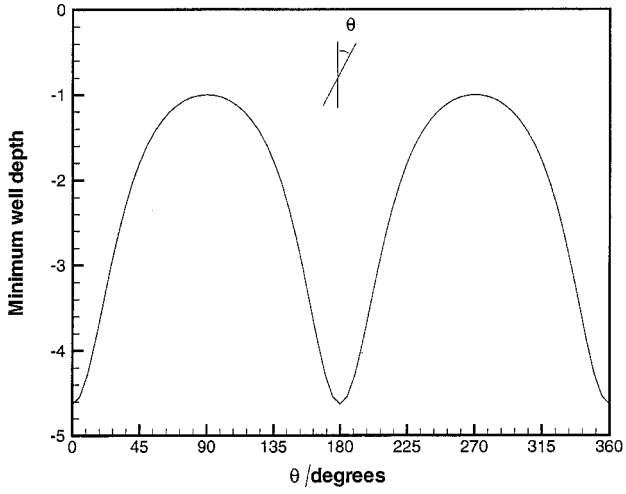

(*b*)

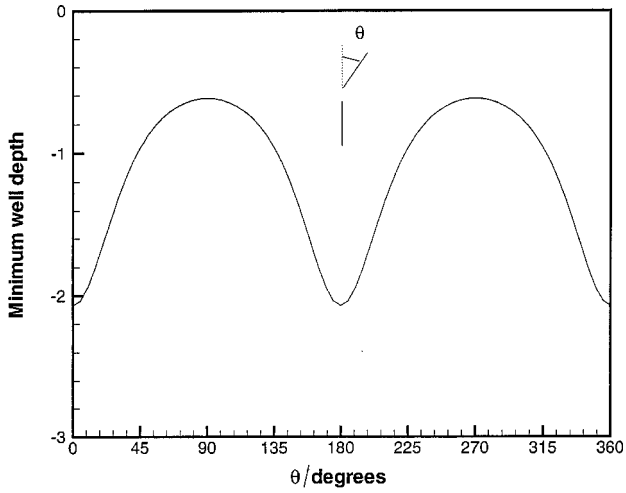

(*c*)

Figure 9. The same as figure 7 but for Gay–Berne molecules with parameters $\sigma_\perp = 1.0$, $\sigma_\parallel = 3.0$.

Specifically, the splay and bend flexoelectric coefficients in the Nemstov–Osipov formalism are given by

$$e_{11} = -E_{\alpha\beta\gamma} e_{\mu\beta\gamma} n_\alpha n_\mu / 2$$
$$e_{33} = E_{\alpha\beta\gamma} e_{\alpha\beta\mu} n_\gamma n_\mu / 2 \tag{15}$$

where we use the summation convention over the Greek indices (summed over the coordinate directions x, y and z). The tensor $e_{\alpha\beta\gamma}$ is the antisymmetric Levi–Civita tensor, while the antisymmetric tensor $E_{\alpha\beta\gamma}$ is the response function satisfying

$$P_\alpha = E_{\alpha\beta\gamma} \gamma_{\beta\gamma} \tag{16}$$

where $\gamma_{\alpha\beta}$ is the orientational strain tensor given by

$$\gamma_{\alpha\beta} = \frac{\partial \theta_\alpha}{\partial x_\beta}. \tag{17}$$

Here θ_α denotes the rotation angle of the director about the coordinate axis labelled by α. For small director deformations $\delta\hat{\mathbf{n}}$, $\theta \sim \sin\theta \sim \hat{\mathbf{n}} \times \delta\hat{\mathbf{n}}$, which then yields

$$\gamma_{\beta\gamma} = e_{\beta\mu\nu} n_\mu \frac{\partial n_\nu}{\partial x_\gamma}. \tag{18}$$

Symmetry considerations show that $E_{\alpha\beta\gamma}$ has four independent components in the nematic and smectic A phases.

Using the fluctuation-dissipation theorem the components of the response function $E_{\alpha\beta\gamma}$ are given by correlation functions of the orientational stress tensor and polarization:

$$E_{\alpha\beta\gamma} = -\frac{\beta}{V} \langle \pi_{\beta\gamma} \mathscr{P}_\alpha \rangle . \tag{19}$$

Here $\beta = 1/k_B T$, V is the volume of the system, $\mathscr{P} = \Sigma_i \boldsymbol{\mu}_i$, ($\boldsymbol{\mu}_i$ is the dipole moment of molecule i), and $\pi_{\alpha\beta}$ is the static orientational stress tensor given by

$$\pi_{\alpha\beta} = \frac{1}{2} \sum_{i \neq j} r_{ij\beta} \tau_{ij\alpha}. \tag{20}$$

In equation (20) r_{ij} is the relative position vector of molecules i and j, and τ_{ij} is the torque exerted by molecule j on i.

In our simulations, then, we calculate the components $E_{\alpha\beta\gamma}$ of the response function by computing the correlation functions in equation (19) as time averages (or MC cycle averages) and then calculate e_{11} and e_{33} from equation (15) (the director is also computed during the simulations). We set the magnitude of the molecular dipole moment to unity; its direction is given by $\hat{\mathbf{u}}$, the long axis of the wedge. The torque on molecule i due to

our generalized potential U_{tot} is given by [19],

$$\tau_i = \sum_{i \neq j} \tau_{ij} = \hat{\mathbf{u}}_i \times (-\nabla_{\hat{\mathbf{u}}} U_{\text{tot}}). \tag{21}$$

4. Results

We performed constant temperature and pressure (with $P^* = P\sigma_o^3/\varepsilon_o = 10$) Monte Carlo simulations on systems of 256 wedges, using the two sets of molecular parameters described in § 2. The systems were equilibrated for 250 000–500 000 cycles and cooled in dimensionless temperature steps of 0.1 (the dimensionless temperature is defined by $T^* \equiv k_B T/\varepsilon_o$). As in [15] we found a strong preference for the system to form a smectic A phase, even when the attractive part of the potential was removed (in the ordinary GB system, removal of the attractive forces tends to stabilize the nematic phase [20]). The use of a different set of Gay–Berne parameters for the attractive portion of the potential [21] (which enhance the stability of the nematic phase for a system of GB ellipsoids) did not stabilize the nematic phase in the present case of wedge-like molecules—another indication that the repulsive core shape is the dominant factor in the possible formation of a nematic phase.

Stelzer *et al.* [15] found that the nematic phase is absent for dipole moment $p^* = 0.814$, though they were able to produce nematic phases over narrow temperature ranges for $p^* = 0.524$ and 0.662. Thus, our inability to produce a stable nematic phase for our molecules with $p^* = 1.38$ is consistent with [15], but our inability to produce a stable nematic for our less asymmetric shape with $p^* = 0.565$ is not; the reason for this discrepancy is not clear. We note that experimentally the splay and bend flexoelectric coefficients in the nematic and smectic phases have been found to be virtually identical [6], while the additional flexoelectric coefficient which appears in the smectic A phase but not in the nematic is negligibly small. Thus, we proceeded to measure the splay and bend flexoelectric coefficients in the smectic phase using the method outlined in § 3.

Interestingly, the smectic layers show a distinct domain structure, see figure 10(*a*). Each domain is characterized by a non-zero splay of the same sign, but the net direction of the orientation vectors $\hat{\mathbf{u}}$ whose heads correspond to the wide ends of the wedges flips from one domain to the next. This domain structure is not observed in the Gay–Berne smectic, figure 10(*b*). Recall from figures 7(*a*) and 8(*a*), that neighbouring wedges prefer splay. The alternation of the net direction of the molecular orientation vectors between domains maintains parallel smectic layers and zero net electric polarization. Note that this domain structure occurs in the absence of an externally applied elastic deformation or electric field. While on average there is no spontaneous splay in the system, there is local spontaneous splay. This local splay is thermally activated and should be expected to appear in a system that exhibits splay flexoelectricity. It represents the essential physics of the fluctuation-dissipation theorem that relates the flexoelectric coefficients (that would be measured in the presence of an external field) to the thermal fluctuations of the director.

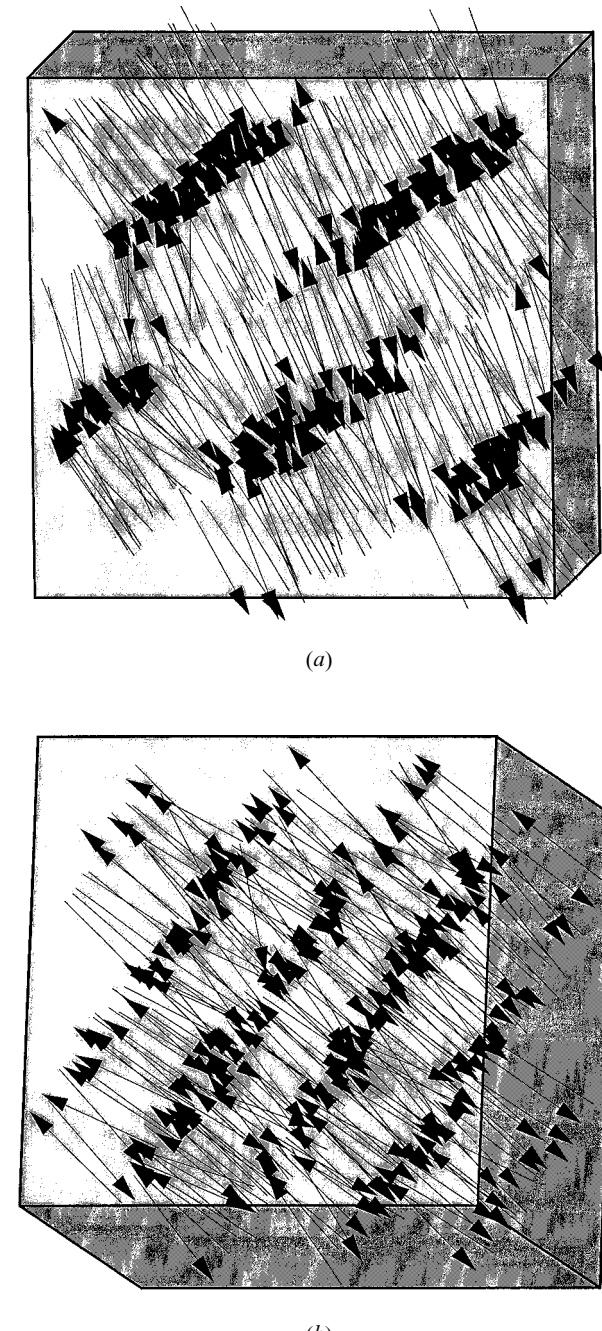

(*a*)

(*b*)

Figure 10. View of the molecular configurations in the smectic layers for (*a*) wedges and (*b*) standard Gay–Berne ellipsoids. The arrows indicate the direction of the orientation vectors $\hat{\mathbf{u}}$ whose heads correspond to the wide ends of the wedges. The domains in the wedge case can be clearly seen.

Table. Flexoelectric coefficients for the small ($p^* = 0.565$) and large ($p^* = 1.38$) wedges and for Gay–Berne ellipsoids. Data for the small wedge was obtained in the isotropic phase at $T^* = 3.5$ and in the smectic phase at $T^* = 2.9$; corresponding values for the large wedge were 2.5 and 1.9. Data for the Gay–Berne ellipsoids were obtained in the smectic phase at $T^* = 0.745$ and $P^* = 2.5$. The nematic order parameter in each of the smectic phases was 0.9.

Molecular shape, phase	e_{11}	e_{33}
Small wedge, isotropic phase	0.367 ± 0.522	− 0.394 ± 0.383
Large wedge, isotropic phase	− 1.39 ± 1.15	0.148 ± 0.251
Gay-Berne ellipsoids, nematic phase	− 0.394 ± 0.581	− 0.0835 ± 0.117
Small wedge, smectic phase	− 2.08 ± 0.211	− 0.061 ± 0.054
Large wedge, smectic phase	13.6 ± 0.052	− 0.005 ± 0.012

Data for the small ($p^* = 0.565$) and large ($p^* = 1.38$) wedges and for Gay–Berne ellipsoids are shown in the table. The Gay–Berne ellipsoids interact via the rod potential equation (3) with parameters $\sigma_\perp = 1.0$, $\sigma_\parallel = 3.0$, $\mu = 2$, and $\nu = 1$. We note that the values of the flexoelectric coefficients for the system of ellipsoids are zero to within the computed error; thus, in accord with Meyer's ideas, this system of symmetric objects does not exhibit flexoelectricity. In the isotropic phase both the large and small wedges also exhibit no flexoelectricity. However, in the smectic phases of both wedges splay flexoelectricity appears. Note the difference in sign between the e_{11} data in the smectic phase for the large and small wedges, consistent with their opposite splays. The actual values for the signs also are as expected: considering again figure 1 with the director $\hat{\mathbf{n}}$ taken to point upwards, the splay shown is then positive and the resulting polarization is parallel to $\hat{\mathbf{n}}$, implying that $e_{11} > 0$, see equation (1); this is the case for the large wedge. For the small wedge, the splay is negative but the polarization is still parallel to $\hat{\mathbf{n}}$, implying $e_{11} < 0$ as observed. The magnitude of e_{11} is also larger for the large wedge, consistent with Meyer's excluded volume mechanism for flexoelectricity. The average values for e_{33}, the bend flexoelectric coefficient, are much smaller in the smectic phases than the corresponding e_{11} values and are zero to within the computed error. This result is consistent with the uniaxial symmetry of our wedges and is a simple check of our approach to calculating flexoelectric coefficients. We also note that the bend coefficients varied in sign over the course of the simulation whereas the values of e_{11} maintained a consistent sign during the runs.

5. Conclusion

By simulating a system of wedge-like molecules formed from Gay–Berne ellipsoids and Lennard–Jones spheres we have explored some of the molecular origins of flexoelectricity. We measured both the bend and splay flexoelectric coefficients using linear response theory, which yields the coefficients in terms of correlation functions of the molecular torque and orientation vector. We studied wedges with two different parametrizations, and found a close connection between the properties of the intermolecular potential and the flexoelectric response of the system. In particular, wedge-shaped molecules do not produce a measurable bend flexoelectric coefficient, and a more prominent wedge-shaped object produces a larger splay flexoelectric coefficient, in accord with Meyer's original ideas on the origins of flexoelectricity. In the case of the less prominently shaped wedge we have obtained a splay flexoelectric coefficient with the opposite sign to that of the more prominent wedge due to the attractive tail of the intermolecular potential and the relative narrowness of the molecular head.

We are grateful to Prof. G. Crawford for helpful discussions. Computational work in support of this research was performed at the Theoretical Physics Computing Facility at Brown University. This work was supported by the National Science Foundation under grants DMR9528092 and DMR9873849.

References

[1] Meyer, R. B., 1969, *Phys. Rev. Lett.*, **22,** 918.
[2] Prost, J., and Marcerou, J. P., 1977, *J. Phys., Paris*, **38,** 315.
[3] Skaldin, O. A., and Chuvyrov, A. N., 1990, *Sov. Phys. Crystallogr.*, **35,** 605.
[4] Marcerou, J.-P., and Prost, J., 1980, *Mol. Cryst. liq. Cryst.*, **58,** 259.
[5] Marcerou, J. P., and Prost, J., 1978, *Ann. Phys.*, **3,** 262.
[6] Prost, J., and Pershan, P. S., 1976, *J. appl. Phys.*, **47,** 2298.
[7] Murthy, P. M., Raghunathan, V., and Madhusudana, N., 1993, *Liq. Cryst.*, **14,** 483.
[8] De Gennes, P. G., 1969, *J. Phys., Paris*, **30,** C4-65.
[9] De Gennes, P. G., and Prost, J., 1993, *The Physics of Liquid Crystals* (Oxford: Clarendon Press).
[10] Fournier, J. B., and Durand, G., 1992, *J. Phys. II Fr.*, **2,** 1001.
[11] Straley, J. P., 1976, *Phys. Rev. A*, **14,** 1835.
[12] Osipov, M. A., 1983, *Sov. Phys. JETP*, **58,** 1167.
[13] Helfrich, W., 1971, *Z. Naturforsch.*, **26A,** 833.
[14] Derzhanski, A., and Petrov, A. G., 1971, *Phys. Lett.*, **36A,** 483.

[15] Stelzer, J., Berardi, R., and Zannoni, C., 1999, *Chem. Phys. Lett.*, **299,** 9.
[16] Cleaver, D. J., Care, C. M., Allen, M. P., and Neal, M. P., 1996, *Phys. Rev. E*, **54,** 559.
[17] Gay, J. G., and Berne, B. J., 1981, *J. chem. Phys.*, **74,** 3316.
[18] Nemtsov, V. B., and Osipov, M. A., 1986, *Sov. Phys. Crystallogr.*, **31,** 125.
[19] Luckhurst, G. R., Stephens, R. A., and Phippen, R. W., 1990, *Liq. Cryst.*, **8,** 451.
[20] De Miguel, E., Rull, L. F., and Gubbins, K. E., 1992, *Phys. Rev. A*, **45,** 3813.
[21] Berardi, R., Emerson, A. J. P., and Zannoni, C., 1993, *J. chem. Soc. Faraday Trans.*, **89,** 4069.
[22] McGrother, S. C., Sear, R. P., and Jackson, G., 1997, *J. chem. Phys.*, **106,** 7315.